Available online at www.sciencedirect.com
ScienceDirect
Journal of Molecular Catalysis A: Chemical 265 (2007) 42–49
JOURNAL OF MOLECULAR CATALYSIS A: CHEMICAL
www.elsevier.com/locate/molcata

pH induced size-selected synthesis of PtRu nanoparticles, their characterization and electrocatalytic properties

Dongsheng Geng [a,b], Liang Chen [a,b], Gongxuan Lu [a,*]

[a] *State Key Laboratory for Oxo Synthesis and Selective Oxidation, Lanzhou Institute of Chemical Physics, Chinese Academy of Sciences, Lanzhou 730000, China*
[b] *Graduate University of Chinese Academy of Sciences, Beijing 100049, China*

Received 23 August 2006; received in revised form 22 September 2006; accepted 22 September 2006
Available online 29 September 2006

Abstract

PtRu/C nanocatalysts with different size were prepared simply by adjusting the pH of β-D-glucose solution. Herein, β-D-glucose acts as a reducing agent as well as a capping agent. Transmission electron microscopy revealed that the well dispersed PtRu particles (12.7, 5.6, and 2.3 nm) were obtained at pH 8.5, 10.5, and 12.5, respectively. X-ray diffraction analysis indicated that the PtRu/C catalysts have different structures synthesized at different pH values. Only at pH 12.5, small amount of PtRu alloy was formed. X-ray photoelectron spectroscopy measurements showed that a large amount of Pt and Ru were present in metallic states. Both cyclic voltammetry and chronoamperometric results demonstrated that the PtRu/C catalyst prepared from the solution at pH 12.5 exhibited better performances for methanol electro-oxidation than the other samples.

Keywords: PtRu/C nanocatalyst; β-D-Glucose; Methanol electro-oxidation; Particle size

1. Introduction

PtRu bimetal particles are electrocatalytically active in fuel cell applications. It is well known that the catalytic activity of metal particle is strongly dependent on their shape, structure, size and size distribution [1–12]. PtRu particles with diameter about 3.0 nm displayed the highest mass catalytic activity for methanol electro-oxidation [13]. Bock et al. [14] reported that particular PtRu catalysts with the size in the range of 1.2–4 nm display the enhanced activity for methanol electro-oxidation reaction (MOR) compared to commercial catalysts. Therefore, the metal particles with high electrocatalytic activity should have suitable size. However, conventional preparation techniques based on wet impregnation and chemical reduction of metal precursors cannot provide satisfied control of particle size. Thus, it is an important and also a challenge work to prepare the bimetal particles with a suitable and uniform size for high performance catalysts.

At present, the colloidal and microemulsion methods are widely used for synthesizing metal nanoparticle with controlled size [15–20]. Microemulsion method may offer unique flexibility in the simultaneous control of the size and the composition of mixed metal nanoparticles. Nevertheless, it requires the use of costly surfactant molecule with extra washing steps, and may not be economical for a large scale synthesis. Although colloidal methods have the advantage to produce very small and homogeneously distributed carbon-supported metal nanoparticles, the preparation is very complex. Therefore, the search for alternative routes to produce metal nanoparticles by a simple methodology is a goal in this area. Recently, the alternative route based on the "polyol method" and "glucose reduction process" has been developed. Chen et al. and Bock et al. [14,21] reported that Pt and PtRu nanoparticles with different mean sizes were synthesized by heating ethylene glycol solution of metal salt at different pH. Daimon and Kurobe [22] also reported that addition of non-metallic elements such as N, P and S reduced the particle size of PtRu catalyst deposited on a carbon support using ethylene glycol as a reductant. In addition, Liu et al. [23] have reported that relatively monodisperse Au nanocrystals with an average diameter of 8.2 nm were synthesized by using nontoxic and renewable biochemical β-D-glucose simply

* Corresponding author. Tel.: +86 931 4968178; fax: +86 931 4968178.
E-mail address: gxlu@lzb.ac.cn (G. Lu).

1381-1169/$ – see front matter © 2006 Elsevier B.V. All rights reserved.
doi:10.1016/j.molcata.2006.09.041

by adjusting the pH in aqueous medium. This method is economically viable and relative "green" as compared to the "polyol method".

In this work, a simple, economically viable and relative "green" approach has been reported for the synthesis of PtRu nanoparticle supported on activated carbon using β-D-glucose aqueous. By adjusting pH value, PtRu nanoparticles with the selected size were obtained. PtRu/C nanocatalysts were characterized using X-ray diffraction (XRD), X-ray photon spectroscopy (XPS), and transmission electron microscopy (TEM). The activities of carbon-supported PtRu particles for the electrochemical CO and CH_3OH oxidation reaction were also studied in detail.

2. Experimental

2.1. Synthesis of PtRu/C catalysts

The preparation of PtRu (1:1) (10 wt.%) on Vulcan XC-72 carbon was carried out in glucose solutions in the presence of H_2PtCl_6 and $RuCl_3$ precursor salts at different pH at 100 °C. Typically, 8.75 mL aqueous solution of 3.86×10^{-3} mol L^{-1} H_2PtCl_6 and 4.5 mL aqueous solution of 7.52×10^{-3} mol L^{-1} $RuCl_3$ were added into 16.75 mL glucose solution, and then an appropriate amount of Vulcan XC-72 carbon (Cabot) was added and ultrasonicated for 30 min in a 100 mL flask. Then, the pH value was adjusted by dropping 0.5 mol L^{-1} NaOH under stirring. Subsequently, the solutions were heated under reflux at 100 °C for 3 h, and then cooled to the room temperature. The carbon-supported PtRu catalysts were then filtered and extensively washed with water and ethanol. The resulted catalysts were dried at 100 °C in air for 2 h. PtRu/C catalysts synthesized at pH 8.5, 10.5, and 12.5 were marked as PtRu/C-1, PtRu/C-2, and PtRu/C-3, respectively.

2.2. Physical characterization

The morphologies and sizes of PtRu/C catalysts were characterized by transmission electron microscopy (JEM1200EX). Sample preparation for TEM examination involved the ultrasonic dispersion of the sample in ethanol and placing a drop of the suspension on a copper grid covered with perforated carbon film. The mean particle size and distribution were obtained from a few randomly chosen areas in the TEM images containing about 150 particles. X-ray photoelectron spectroscopy was carried out using a VG ESCALAB 210 electron spectrometer with Mg Kα radiation. A Philips X'Pert diffractometer was used to obtain the power X-ray diffraction patterns using Cu Kα radiation.

2.3. Electrochemical measurements

CHI 660A electrochemistry workstation and a three-compartment cell were employed for the electrochemical measurement. Glassy carbon (GC) with an area 0.07 cm^2 is used for the working electrode. Pt wire and saturated calomel electrode (SCE) were used as the counter and reference electrode, respectively. All potentials in this study are reported with respect to SCE. The PtRu/C loading on the GC is 15 μg cm^{-2}. Voltammetry experiments were performed in 0.5 M NaOH solution containing 1 M CH_3OH at a scan rate of 50 mV s^{-1}. N_2 gas was purged for nearly 30 min before starting the experiment. In all the experiments, stable voltammogram curves were recorded after scanning for seven cycles in the potential region from −1.0 to 0.4 V in 0.5 M NaOH solution. Chronoamperometry (current versus time response) tests were conducted using a three-electrode cell in 0.5 M NaOH solution containing 1 M CH_3OH at −0.3 V for the period of 1000 s. For CO-stripping measurement, pre-adsorption of CO on the electrode catalyst was carried out by bubbling carbon monoxide through the electrolyte for 20 min followed by purging with nitrogen for 30 min to remove any residual CO in the solution.

3. Results and discussion

3.1. PtRu particle synthesized in glucose solution

The synthesis of monometallic noble metal colloids in glucose solution has been suggested in previous works [23–25]. It was proposed that glucose could stabilize the Pt nanoparticles and glucose act both as reducing agent and capping agent for the synthesis and stabilization of Au nanoparticles in alkaline environment at room temperature. In our experiments, it was observed that recovered glucose solution was colorless. This fact indicated that the reactions were complete and all of PtRu particles should almost be deposited on carbon surface. We also found that PtRu particles could not be synthesized at acidic and neutral solutions. So it is believed that OH^- ions are involved in the reaction to yield PtRu nanoparticle. The reduction reaction equation [23] was shown in Scheme 1. Here, the five hydroxyls groups in the glucose molecule can facilitate the complexation sites for the PtRu nanoparticles to the molecular matrix

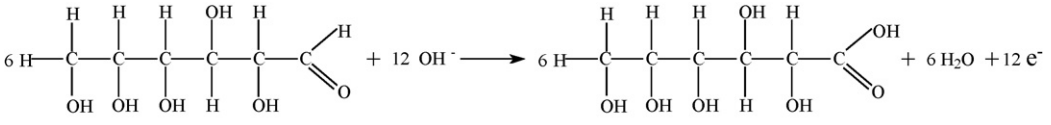

$$3\ Pt^{4+} + 12\ e^- \rightarrow 3\ Pt^\circ$$
$$4\ Ru^{3+} + 12\ e^- \rightarrow 4\ Ru^\circ$$

Scheme 1. The reaction equation for the formation of PtRu nanopaticles.

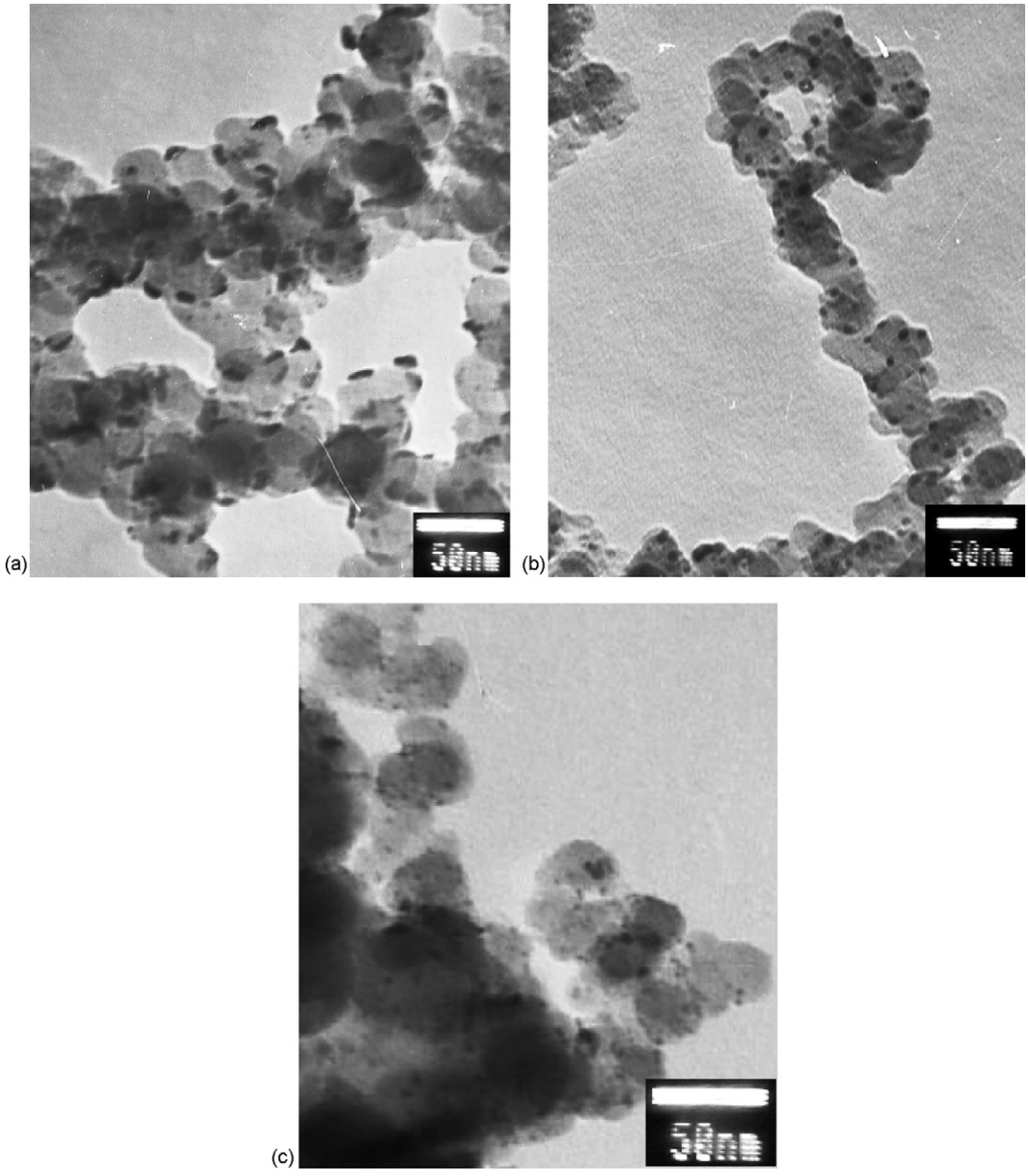

Fig. 1. TEM images of 10 wt.% PtRu/C nanocatalysts: (a) PtRu/C-1; (b) PtRu/C-2; (c) PtRu/C-3.

of glucose. Glucose acts as both reducing agent and capping agent.

3.2. TEM analysis

Fig. 1 presents the TEM images of the PtRu/C nanocatalysts prepared in alkaline glucose solution under different pH values. The corresponding histograms of size distribution are shown in Fig. 2. It can be seen that well-dispersed PtRu nanoparticles were formed on the carbon support and PtRu particles size became smaller and more uniform with the increase of solution pH. The average sizes (and size ranges) were 12.7 (5.3–16), 5.6 (4.5–6.9) and 2.3 nm (1.2–4.0) for pH 8.5, 10.5 and 12.5, respectively. So the pH value of the synthesis solution is a key factor influencing the size and uniformity of PtRu particles. At higher pH values, it was believed that glucose can quickly generate reducing species for the reduction of the metal ions, accelerating the reduction of the metal ions and the formation of metallic nuclei, thus greatly facilitating smaller and more uniform particle formation. In addition, the carbon surface may offer suitable sites for heterogeneous nucleation and inhibit particle growth.

3.3. XRD measurements

Fig. 3 shows the XRD spectra for all the PtRu/C catalysts. Their diffraction peaks were compared with the standard patterns of Pt (JCPDS, card 4-802) and Ru (JCPDS, card 6-663). The diffraction peaks indicate the presence of the face centered cubic (fcc) structure of Pt with representative planes (1 1 1), (2 0 0), (2 2 0), (3 1 1), and (2 2 2). Meanwhile, the peaks asso-

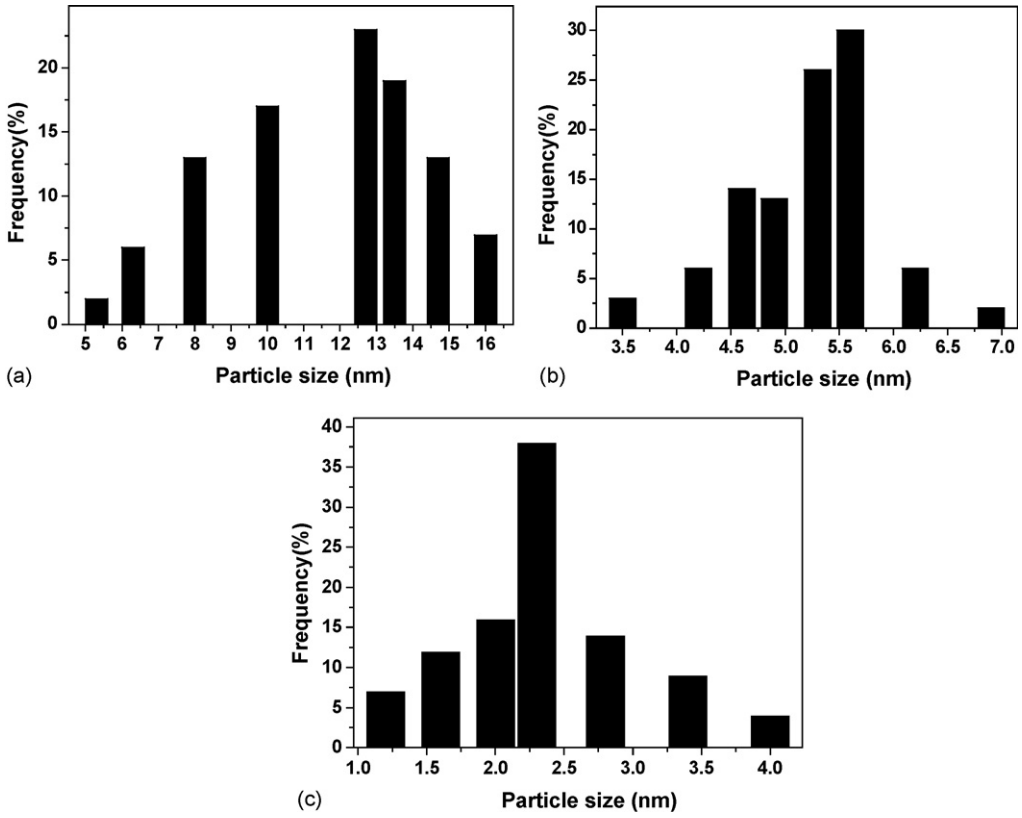

Fig. 2. Histograms of PtRu particle size distribution for (a) PtRu/C-1, (b) PtRu/C-2, and (c) PtRu/C-3.

ciated with a typical hexagonal close-packed (hcp) structure of pure Ru and RuO_2 appeared in the XRD pattern of PtRu/C-1. The peaks of RuO_2 also appeared in the XRD pattern of PtRu/C-2. This indicated the existence of metallic Ru and its oxides (RuO_2) [26,27]. But the intensities of the Ru and RuO_2 reflection was very weak compared to those of the Pt peaks. These results indicated that there were the small amount of coherently scattering Ru particles in the samples. Pt and Ru was found in separate phases. According to previous reports [28–30], the addition of Ru resulted in the broaden PtRu diffraction peak and a shift to higher 2θ values. But our results indicated that none of catalysts, as shown in Fig. 3, is consistent with those phenomena reported for PtRu alloys in literature. The lattice parameter (a_{fcc}) showed the formation of the Pt–Ru alloyed phase in the fcc structure. For PtRu/C-1, PtRu/C-2, and PtRu/C-3 catalysts, the values of a_{fcc} were 3.9191, 3.9182 and 3.9030 Å, respectively. Only the a_{fcc} value of PtRu/C-3 was slightly lower than that of Pt/C (3.9150 Å), which indicated the formation of small amount of PtRu alloy particles. So mainly amorphous state of metallic Ru and its oxides existed in all catalysts. Moreover, it was noted that FWHM (full-width half-maximum) of the XRD peaks of PtRu increased with the increase of the synthesis solution pH. All these facts indicated that PtRu particles size and structure were influenced by the pH of the solution. The difference between structure and size may be related to the different reduction velocity of reaction induced by pH. The average particle size for PtRu/C nanocatalysts was also calculated using Scherrer's equation [6,11,31]. These sizes were consistent with those obtained from TEM results and are given in Table 1.

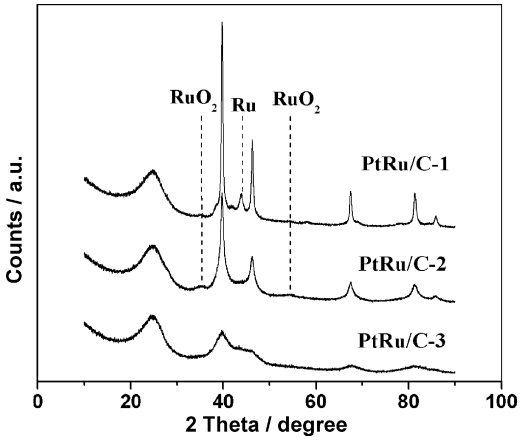

Fig. 3. XRD patterns of all PtRu/C catalysts.

3.4. XPS characterization

The surface compositions and chemical oxidation states of Pt and Ru in the PtRu/C nanocatalysts were determined by XPS analysis. Fig. 4 shows the regional Pt 4f and Ru $3p_{3/2}$ spectra for the PtRu/C-2 nanocatalyst. The Pt 4f spectrum showed a doublet low-energy band (Pt $4f_{7/2}$) and a high-energy band (Pt $4f_{5/2}$) at 71.1 and 74.4 eV, respectively (see Fig. 4a). The lower binding energy value is in good agreement with the literature data of Pt at 71.1 eV [32]. To identify different oxidation states of Pt, the spectrum was de-convoluted into two pairs of peaks at 71.1 and

Table 1
Mean particle size, the electrochemical activity area (EAA) and the highest methanol oxidation current for PtRu/C-1, PtRu/C-2, and PtRu/C-3

PtRu/C under different pH	Average particle size from XRD (nm)	Particle size from TEM (nm)	EAA ($m^2\ g^{-1}$)	I_{peak} (mA)
8.5	12.3	12.7	11.6	0.23
10.5	5.4	5.6	29.1	0.43
12.5	2.1	2.3	55.4	1.03

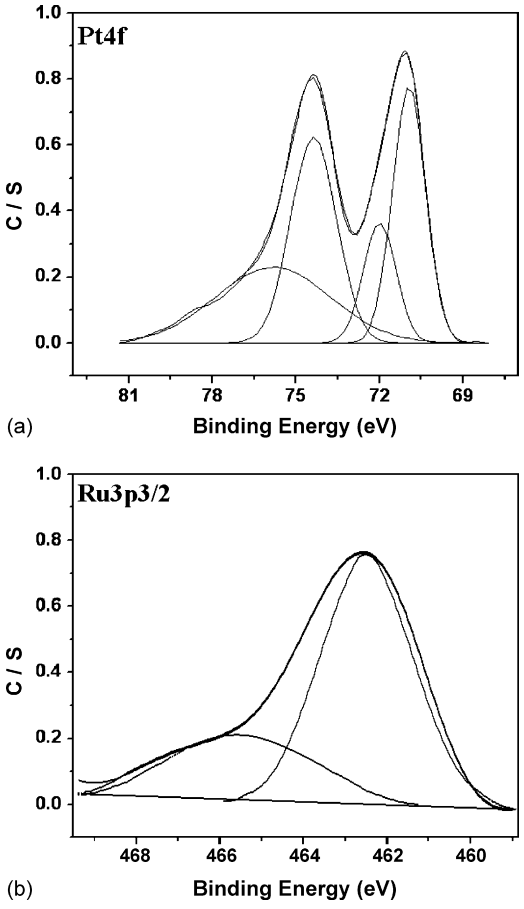

Fig. 4. Regional XPS of (a) Pt 4f and (b) Ru $3p_{3/2}$ spectra for the PtRu/C-2 catalyst.

74.4 and at 72.2 and 75.8 eV. These two pairs of peaks indicated that Pt was present in two different oxidation states, Pt(0) and Pt(II). The amounts of Pt(0) and Pt(II) species were calculated from the relative intensities of these two peaks and were given in Table 2. In the case of Ru, the Ru $3p_{3/2}$ spectrum was deconvoluted instead of the Ru $3d_{3/2}$ spectrum, because the latter always overlaps the C 1s spectrum, which prevents an accurate determination of Ru oxidation states. Thus, one pair of peak Ru $3p_{3/2}$ was obtained as shown in Fig. 4b. The first and second peaks were 462.5 and 465.8 eV, respectively. These values correspond to two different oxidation stations of Ru, namely Ru(0) and Ru(IV). The amounts of Ru species were calculated from the relative intensities of these peaks and were also given in Table 2. Table 2 showed that relatively higher amounts of Pt and Ru were present in their metallic states in the PtRu/C nanocatalysts.

Table 2
Binding energies and relative intensities of different oxidation states of Pt and Ru in the PtRu/C nanocatalyst prepared at pH 10.5

Species	Binding energy (eV)	Relative intensity (%)
Pt(0)	71.1	82.2
Pt(II)	72.2	17.8
Ru(0)	462.5	75.5
Ru(IV)	465.8	24.5

3.5. CO stripping on all PtRu/C catalysts

First, an electro-oxidation reaction of pre-adsorbed CO (CO_{ad}) at PtRu/C catalyst was investigated, because this is a well-known determining step in the MOR. Fig. 5 shows cyclic voltammograms with CO_{ad} (solid curve) and without (dashed curve) CO_{ad} at PtRu/C in 0.5 M NaOH. It can be observed that for all the PtRu/C catalysts the hydrogen adsorption peaks are suppressed in the lower potential region, which is due to the saturated coverage of CO_{ad} species on the Pt sites of these catalysts. For all the catalysts, the onset of CO oxidation is similar at about −0.55 V. However, for PtRu/C-1, PtRu/C-2, and PtRu/C-3, the peak potentials are −0.4, −0.32, and −0.36 V, respectively. This difference can be attributed to the size effect and the presence of heterogeneous phases of Pt, Ru, PtRu and RuO_2 on the surface of the PtRu catalysts. Furthermore, we measured the electrochemically active area (EAA, $m^2\ g^{-1}$) for all the catalysts by using the CO oxidation charge after subtracting the background current of the subsequent CV curves with the assumption of 420 $\mu C\ cm^{-2}$ as the oxidation charge for one monolayer of CO on a smooth Pt surface. The measured EAA values are given in Table 1. It shows that the surface area increases with the increase of the synthesis solution pH, which is not surprising in view of the decrease of the metallic particle size with the pH increase and is in agreement with the previous results [21,33]. The smaller electrochemically active area means that a lower number of Pt atoms is present in the electrode surface.

3.6. Electro-oxidation characteristics of CH_3OH

Fig. 6 shows the cyclic voltammograms of methanol electro-oxidation on glucose solution synthesized PtRu/C catalysts in electrolytes of 0.5 M NaOH/1 M CH_3OH at room temperature. The current peak at about −0.3 V versus SCE in the forward scan is attributed to methanol electro-oxidation. As shown in Fig. 6c, the current peak of methanol electro-oxidation on PtRu/C-3 displays the highest peak current (I_{peak}) among these PtRu/C catalysts. All the peak current values also are given in Table 1. The onset potentials of methanol oxidation for all the catalysts are around −0.6 V. Therefore, the particle size only affects the peak current, but the onset and peak potential.

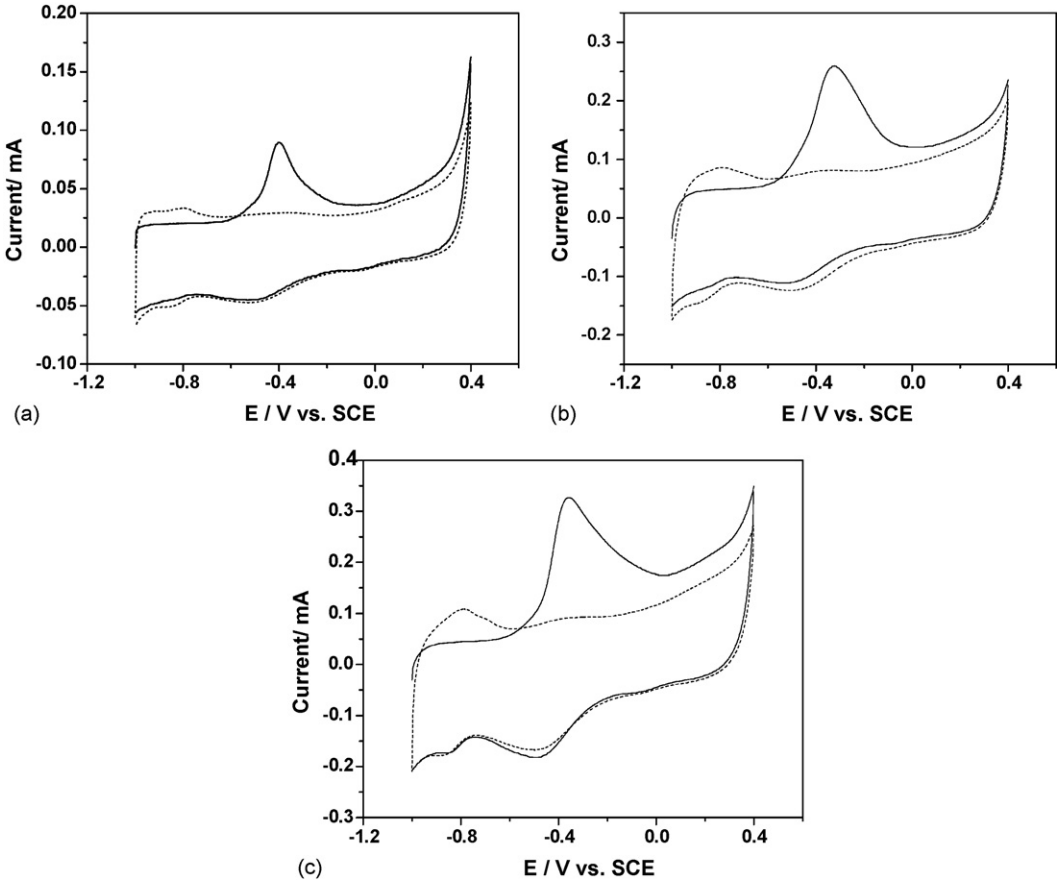

Fig. 5. CO-stripping cyclic voltammograms of (a) PtRu/C-1, (b) PtRu/C-2, and (c) PtRu/C-3 in alkaline (0.5 M NaOH) electrolytes with (solid curve) and without (dashed curve) CO_{ad}. Scan rate 50 mV/s.

In parallel work, chronoamperometry measurements at constant potential (−0.3 V) were carried out over 1000 s periods (Fig. 7). The results show that the catalytic advantage of these PtRu/C catalysts are maintained. It can be seen that PtRu/C-3 exhibits not only higher initial current but also higher current at all corresponding potentials than other samples from Fig. 7. The above facts indicate that PtRu/C-3 displays better performances for methanol electro-oxidation than other samples. It is because that PtRu/C prepared at pH 12.5 has a suitable size and structure.

3.7. Kinetic characterization of methanol electro-oxidation on PtRu/C-3

Fig. 8 shows the effect of methanol concentration on the oxidation reaction for PtRu/C-3 in 0.5 M NaOH at room temperature. Anodic peak current increased with the concentration

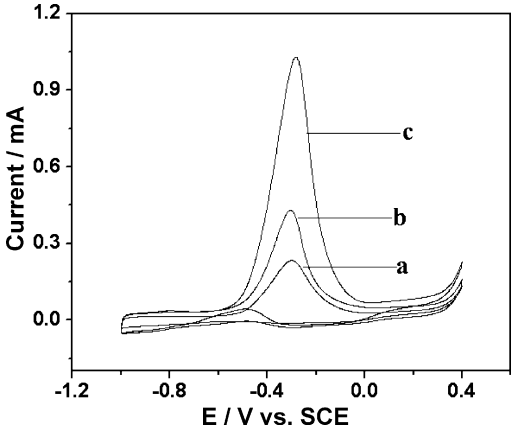

Fig. 6. Cyclic voltammetric curves for all the PtRu/C catalysts with different pH: (a) pH 8.5; (b) pH 10.5; (c) pH 12.5 (on GC electrode, 0.07 cm^2) in alkaline (0.5 M NaOH) electrolytes with 1.0 M methanol. Scan rate 50 mV/s.

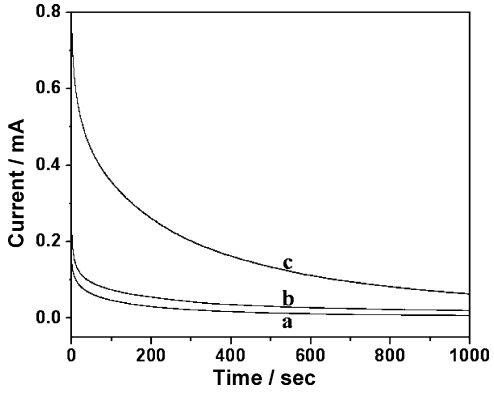

Fig. 7. Chronoamperometric response of all the PtRu/C catalysts with different pH: (a) pH 8.5; (b) pH 10.5; (c) pH 12.5 in 1.0 M methanol solution in 0.5 M NaOH at an applied potential of −0.3 V vs. SCE.

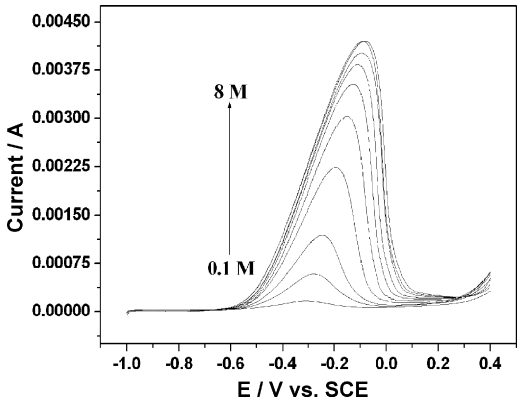

Fig. 8. The linear sweep voltammetry curves for methanol oxidation on PtRu/C-3 at a scan rate of 50 mV s^{-1} at different concentrations: 0.1, 0.5, 1, 2, 3, 4, 5, 6, 7, and 8 M CH_3OH/0.5 M H_2SO_4 electrolyte from inner to outer.

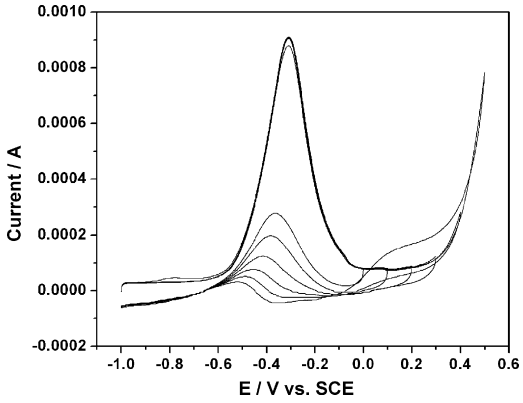

Fig. 10. Cyclic voltammograms of room temperature methanol electrooxidation over PtRu/C-3 at 50 mV s^{-1} in 1 M CH_3OH/0.5 M H_2SO_4 electrolyte for different forward potential scan limit.

of methanol in the region of 0.1–8 M. However, a saturation of the current response was observed at methanol concentration of 7 M. The oxidation of methanol produces CO and possibly other adsorbed intermediates, which can be oxidized with the participation of oxygenated species formed on the surface. The latter process is inhibited by the adsorption of methanol on the surface, which increases with the increase in methanol concentration. Cyclic voltammetry also detected a slow but gradual current decrease with cycling, which is often attributed to the accumulation of strong chemisorbed species on the catalyst surface.

The effect of the scan rate on the electro-oxidation of methanol on PtRu/C-3 is shown in Fig. 9. In the range of 25–200 mV s^{-1}, the peak current increases linearly with the square root of the scan rates (Fig. 9, inset). It shows that the methanol electro-oxidation process on PtRu/C-3 is controlled by the diffusion of methanol to the electrode surface. Additionally, the peak potential (the forward scan) increases with the increase of scan rate. It is indicated that the oxidation of methanol is an irreversible electrode process.

The effect of the potential scan limit on the scan peak current is shown in Fig. 10. The forward scan peak current remained constant on the whole with increasing the anodic limit in the forward scan. The reverse anodic peak potential shifted negatively with increasing the anodic limit in the forward scan, while the peak current decreases. This behavior indicates that the reverse anodic peak current is primarily associated with residual carbon species on the surface of the PtRu/C-3 electrode.

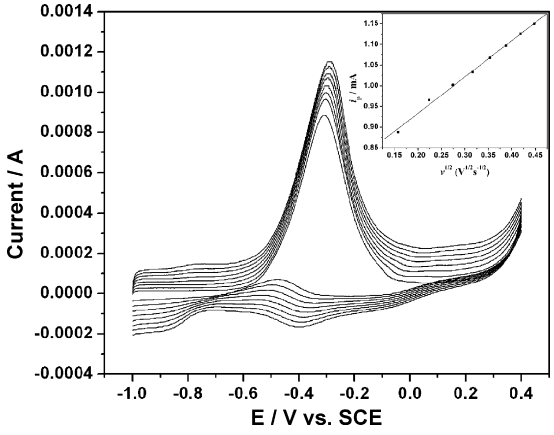

Fig. 9. Voltammograms of 1 M CH_3OH in 0.5 M H_2SO_4 solution. Scan rate: 25, 50, 75, 100, 125, 150, 175, 200 mV s^{-1} from inner to outer. The plot of peak current vs. square root of sweep rates (inset).

4. Conclusions

Size-selected PtRu/C nanocatalysts were synthesized in alkaline glucose solution by simply adjusting the pH. The PtRu particles become smaller and more uniform with the increase of alkaline glucose solution pH. The average sizes (and size ranges) are 12.7 (5.3–16), 5.6 (4.5–6.9) and 2.3 nm (1.2–4.0) for pH 8.5, 10.5 and 12.5, respectively. In addition, XRD measurements indicated that PtRu/C catalysts have the different structure under the different pH. A small amount of PtRu alloy was formed for PtRu/C catalysts only at pH 12.5. CV and CA tests revealed that PtRu/C exhibited better performances for methanol electrooxidation than other samples when the synthesis solution pH was 12.5.

Acknowledgement

The 973 (G20000264) Research Fund is acknowledged for support of the research.

References

[1] F. Maillard, M. Eikerling, O.V. Cherstiouk, S. Schreier, E. Savinova, U. Stimming, Faraday Discuss. 125 (2004) 357.
[2] K.J.J. Mayrhofer, B.B. Blizanac, M. Arenz, V.R. Stamenkovic, P.N. Ross, N.M. Markovic, J. Phys. Chem. B 109 (2005) 14433.
[3] M. Min, J. Cho, K. Cho, H. Kim, Electrochim. Acta 45 (2000) 4211.
[4] L. Dubau, F. Hahn, C. Coutanceau, J.-M. Leger, C. Lamy, J. Electroanal. Chem. 554–555 (2003) 407.
[5] T. Page, R. Johnson, J. Hormes, S. Noding, B. Rambabu, J. Electroanal. Chem. 485 (2000) 34.
[6] V. Radmilović, H.A. Gasteiger, R.N. Ross Jr., J. Catal. 154 (1995) 98.
[7] H. Hoster, T. Iwasita, H. Baumgärtner, W. Vielstich, Phys. Chem. Chem. Phys. 3 (2001) 337.
[8] Z. Tang, D. Geng, G. Lu, J. Colloid Interf. Sci. 287 (2005) 159.

[9] S. Park, Y. Xie, M.J. Weaver, Langmuir 18 (2002) 5792.
[10] E. Antolini, Mater. Chem. Phys. 78 (2003) 563.
[11] J.W. Guo, T.S. Zhao, J. Prabhuram, R. Chen, C.W. Wong, Electrochim. Acta 51 (2005) 754.
[12] T. Iwasita, H. Hoster, A. John-Anacker, W.F. Lin, W. Vielstich, Langmuir 16 (2000) 522.
[13] Y. Takasu, H. Itaya, T. Iwazaki, R. Miyoshi, T. Ohnuma, W. Susimoto, Chem. Commun. (2001) 341.
[14] C. Bock, C. Paquet, M. Couillard, G.A. Botton, B.R. MacDougall, J. Am. Chem. Soc. 126 (2004) 8028.
[15] H. Bönnemann, R.M. Richards, Eur. J. Inorg. Chem. 10 (2001) 2455.
[16] A. Roucoux, J. Schulz, H. Patin, Chem. Rev. 102 (2002) 3757.
[17] K.-Y. Chan, J. Ding, J. Ren, S. Cheng, K.Y. Tsang, J. Mater. Chem. 14 (2004) 505.
[18] H. Liu, C. Song, L. Zhang, J. Zhang, H. Wang, D.P. Wilkinson, J. Power Sources 155 (2006) 95.
[19] X. Zhang, K.-Y. Chan, Chem. Mater. 15 (2003) 451.
[20] L. Xiong, A. Manthiram, Solid State Ionics 176 (2005) 385.
[21] X. Li, W.-X. Chen, J. Zhao, W. Xing, Z.-D. Xu, Carbon 43 (2005) 2168.
[22] H. Daimon, Y. Kurobe, Catal. Today 111 (2006) 182.
[23] J. Liu, G. Qin, P. Raveendran, Y. Ikushima, Chem. Eur. J. 12 (2006) 2131.
[24] J. Liu, P. Raveendran, G. Qin, Y. Ikushima, Chem. Commun. (2005) 2972.
[25] S. Panigrahi, S. Kundu, S.K. Ghosh, S. Nath, T. Pal, Colloids Surf. A 264 (2005) 133.
[26] A.H.C. Sirk, J.M. Hill, S.K.Y. Kung, V.I. Birss, J. Phys. Chem. B 108 (2004) 689.
[27] C. Bock, M.-A. Blakely, B. MacDougall, Electrochim. Acta 50 (2005) 2401.
[28] Y. Lin, X. Cui, C.H. Yen, C.M. Wai, Langmuir 21 (2005) 11474.
[29] E. Antolini, F. Cardellini, J. Alloys Compd. 315 (2001) 118.
[30] C. Both, N. Marlang, H. Fuess, Phys. Chem. Chem. Phys. 3 (2001) 315.
[31] Z. Liu, J.Y. Lee, W. Chen, M. Han, L.M. Gan, Langmuir 20 (2004) 181.
[32] C.D. Wagner, W.M. Riggs, L.E. Davis, J.F. Moulder, Handbook of X-ray Photoelectron Spectroscopy, Perkin-Elmer Corp., Eden Prairie, MN, 1978.
[33] Y. Verde, G. Alonso-Nuñez, M. Miki-Yoshida, M. José-Yacamán, V.H. Ramos, A. Keer, Catal. Today 107–108 (2005) 826.